The Plant Cell, Vol. 9, 1445–1457, August 1997 © 1997 American Society of Plant Physiologists

Actin Purified from Maize Pollen Functions in Living Plant Cells

Haiyun Ren,[a,1] Bryan C. Gibbon,[a] Sharon L. Ashworth,[a] Debra M. Sherman,[b] Ming Yuan,[a,2] and Christopher J. Staiger[a,3]

[a] Department of Biological Sciences, Purdue University, West Lafayette, Indiana 47907
[b] Department of Botany and Plant Pathology, Purdue University, West Lafayette, Indiana 47907

A vast array of actin binding proteins (ABPs), together with intracellular signaling molecules, modulates the spatiotemporal distribution of actin filaments in eukaryotic cells. To investigate the complex regulation of actin organization in plant cells, we designed experiments to reconstitute actin–ABP interactions in vitro with purified components. Because vertebrate skeletal α-actin has distinct and unpredictable binding affinity for nonvertebrate ABPs, it is essential that these in vitro studies be performed with purified plant actin. Here, we report the development of a new method for isolating functional actin from maize pollen. The addition of large amounts of recombinant profilin to pollen extracts facilitated the depolymerization of actin filaments and the formation of a profilin–actin complex. The profilin–actin complex was then isolated by affinity chromatography on poly-L-proline–Sepharose, and actin was selectively eluted with a salt wash. Pollen actin was further purified by one cycle of polymerization and depolymerization. The recovery of functional actin by this rapid and convenient procedure was substantial; the average yield was 6 mg of actin from 10 g of pollen. We undertook an initial physicochemical characterization of this native pollen actin. Under physiological conditions, pollen actin polymerized with kinetics similar in quality to those for vertebrate α-actin and had a critical concentration for assembly of 0.6 μM. Moreover, pollen actin interacted specifically and in a characteristic fashion with several ABPs. Tradescantia cells were microinjected and used as an experimental system to study the behavior of pollen actin in vivo. We demonstrated that purified pollen actin ameliorated the effects of injecting excess profilin into live stamen hair cells.

INTRODUCTION

The eukaryotic actin cytoskeleton provides a dynamic framework for many fundamental cellular processes and has been implicated in changes of the cytoarchitecture in response to internal and external signals. Numerous studies have documented dramatic changes in the spatiotemporal distribution of filamentous actin (F-actin) in dividing and differentiating higher plant cells (reviewed in Meagher, 1991; Staiger and Lloyd, 1991; Hepler et al., 1993; Meagher and Williamson, 1994). These cytological data, in combination with results from the use of pharmacological agents that disrupt actin organization, give us a fairly broad picture of actin's role in higher plants. It is now generally accepted that F-actin participates in cytoplasmic streaming, organelle and nuclear positioning, cellular morphogenesis, and cell division. Further elucidation of the molecular details of cytoskeletal function will require a combination of biochemical, genetic, and cell biological approaches.

Our understanding of how the plant actin cytoskeleton is regulated has been greatly enhanced in recent years by the identification of genes and proteins for actin and several actin binding proteins (ABPs; reviewed in Meagher and McLean, 1990; McCurdy and Williamson, 1991; Meagher, 1991; Staiger et al., 1997). The unique constellation of ABPs in each cell probably confers both functional and organizational properties on the cytoskeleton and allows for rapid responses to intracellular and environmental stimuli. A common approach for dissecting the interaction of ABPs with actin is to approximate the in vivo conditions by combining purified components in vitro. Most physicochemical studies of plant ABPs have used the most readily available source of eukaryotic actin, the rabbit skeletal muscle α-actin isoform (RSMA), and bacterially expressed plant ABPs (Giehl et al., 1994; Lopez et al., 1996; Perelroizen et al., 1996; Carlier et al., 1997). Although studies that have used heterologous components provide compelling evidence that plant ABPs are indeed functional, many important subtleties may be either lost or misinterpreted. For example, yeast actin and RSMA share 87% amino acid sequence identity, yet their polymerization properties and interaction with yeast profilin differ substantially

[1] Current address: Department of Biology, Beijing Normal University, Beijing 100875, China.
[2] Current address: Department of Biological Sciences, Beijing Agriculture University, Beijing 100094, China.
[3] To whom correspondence should be addressed at 1392 Lilly Hall of Life Sciences, Department of Biological Sciences, Purdue University, West Lafayette, IN 47907-1392. E-mail cstaiger@bilbo.bio.purdue.edu; fax 765-496-1496.

(Nefsky and Bretscher, 1992; Kim et al., 1996). Plants contain multigene families for diverse actins that share 83 to 89% amino acid sequence identity with other eukaryotic actins (Meagher and McLean, 1990; Meagher, 1991; Meagher and Williamson, 1994). The multigene families for profilin and the actin depolymerizing factor show even less conservation; 25 to 40% identity with eukaryotic counterparts is typical (Staiger et al., 1997). Thus, further understanding of plant actin function in vivo and in vitro will require a detailed analysis of ABP–actin interactions with physiologically relevant partners.

Analysis of the physicochemical properties of plant ABPs has been greatly facilitated by the ability to overexpress recombinant proteins in bacteria (e.g., Giehl et al., 1994; Lopez et al., 1996; Perelroizen et al., 1996; Carlier et al., 1997). Unfortunately, this strategy has not been successfully applied to any eukaryotic actin (reviewed in Sheterline et al., 1995). This is partly because of the lack of appropriate molecular chaperones required for proper actin folding (Chen et al., 1994; Vinh and Drubin, 1994) and the inability of actin to refold into a functional form after denaturation (Sheterline et al., 1995). Native actin can be purified from eukaryotic cells and tissues by various combinations of methods that include cycles of assembly/disassembly, anion exchange, gel filtration, and DNase I or profilin affinity chromatography (reviewed in Sheterline et al., 1995). However, studies reporting actin isolation from plants are extremely limited (reviewed in Meagher, 1991; Meagher and Williamson, 1994). In addition to general difficulties with the biochemical isolation of proteins from plant material, the low abundance of actin in many tissues, the presence of proteases, and suspected differences in the affinity of plant actin isoforms for DNase I have hampered efforts to purify large quantities of polymerization-competent plant actin. We report here a new strategy for isolating large amounts of functional plant actin from the pollen of maize and perform an initial characterization of the in vitro and in vivo properties of this protein.

RESULTS

A New Method for Actin Purification

We developed a novel strategy for the rapid, convenient, and reproducible purification of native actin from the pollen of maize. The method takes advantage of the binding affinity of actin and profilin and the ability of poly-L-proline (PLP) to bind the actin–profilin complex. This method requires only a single affinity chromatography step followed by one cycle of polymerization and depolymerization. Figure 1 shows the results from a representative pollen actin isolation procedure. Briefly, a high-speed supernatant was prepared from a 10-g sample of frozen, ungerminated maize pollen (Figure 1A, EX) that was disrupted by grinding and sonication in a buffer modified from Katakami et al. (1992). The supernatant was then supplemented with 20 mg of recombinant human profilin I and applied to a column of PLP–Sepharose. The majority of profilin and pollen actin was depleted from the extract and retained on the matrix, as determined by SDS-PAGE (Figure 1A, FT) and immunoblotting (data not shown). After several column volumes of wash (Figure 1A, W), actin was selectively eluted with 1 M KCl (Figure 1A, fractions 1 to 14). Additional actin and the actin–profilin complexes were eluted with a low-ionic-strength step using buffer G (see Methods; Figure 1A, fractions 17 to 27). The remaining profilin was eluted by steps of 2 and 7 M urea (Figure 1A, fractions 33 to 35 and 43 to 47).

Actin isolated from the affinity column was further purified by a cycle of assembly and disassembly. Fractions from the 1 M KCl and buffer G steps that contained actin were pooled separately, dialyzed, and polymerized at room temperature for several hours by the addition of $MgCl_2$ and KCl to 5 and 100 mM, respectively. F-actin was collected by centrifugation at 100,000*g* for 3 hr. Depolymerization was achieved by resuspending the pellet(s) in low-ionic-strength buffer and extensive dialysis. Before quantification of the yield, nondepolymerized actin and denatured protein were removed by centrifugation. Purified actin can be stored at −75°C in buffer G with only moderate loss of activity. For the biochemical experiments reported in this study, only freshly prepared actin from the 1 M KCl eluate was used.

Yields from this rapid and simple procedure were substantial. From 10 g of maize pollen, affinity chromatography yielded an average (±SD) of 8.3 ± 2.2 mg of actin from the 1 M KCl eluate (n = 6) and an additional several milligrams from the low-ionic-strength eluate. After one cycle of polymerization and depolymerization of the 1 M KCl eluate, the average yield (±SD) was 6.0 ± 1.3 mg of actin (n = 10). The crude extract from 10 g of maize pollen contained 278 ± 4 mg (n = 3) of protein; thus, a low estimate for actin concentration is 2% of total soluble cellular proteins. Purified pollen actin (Figure 1B, lane 1) comigrated with RSMA (Figure 1B, lane 2) and had an apparent M_r of 42 kD. Densitometry of overloaded SDS–polyacrylamide gels, such as those shown in Figure 1B, indicated that the actin was >98% pure and free of high molecular weight contaminants. A monoclonal antibody raised against chicken gizzard actin (Lessard, 1988) recognized pollen actin (Figure 1B, lane 3). Isoelectric focusing under denaturing conditions revealed that the assembly-competent pollen actin is composed of a single major isoform with a pI of 5.4 and several minor actin isoforms or degradation products (Figure 1C, lane 1). The major α-actin isoform of RSMA has a pI of 5.3 (Figure 1C, lane 2).

Properties of Maize Pollen Actin in Vitro

The purified pollen actin was evaluated for assembly kinetics, steady state polymer levels, and ABP interactions in vitro. Actin polymerization was measured by 90° light scattering (Cooper and Pollard, 1982). When 5 μM pollen G-actin

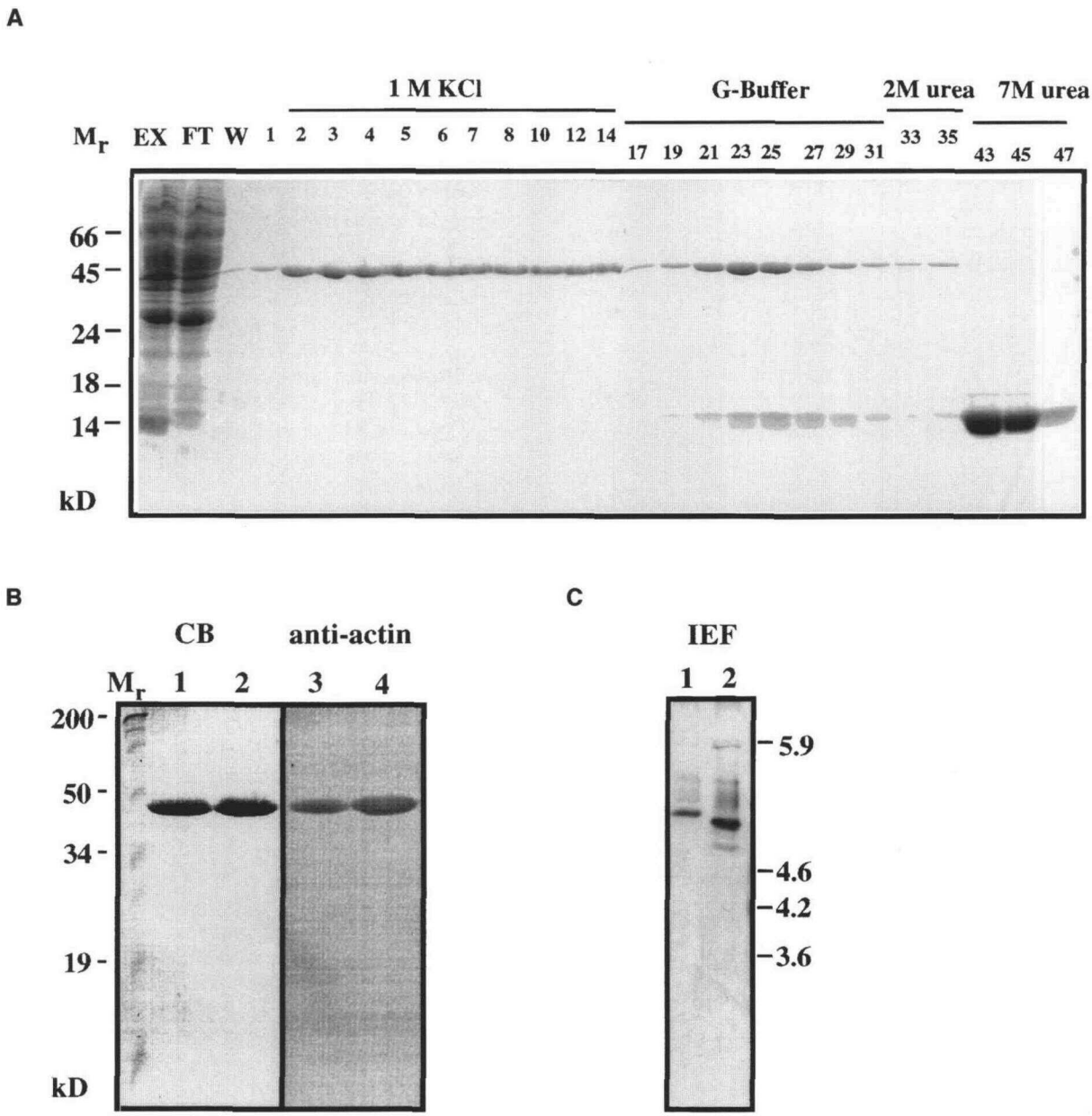

Figure 1. Gel and Immunoblot Analyses of Maize Pollen Actin Purification.

(A) Coomassie blue–stained gel of a representative actin purification experiment. Lanes include molecular mass standards given in kilodaltons. Actin migrates at 42 kD and profilin at 14 kD. EX, clarified pollen extract; FT, flow-through from the PLP–Sepharose column; W, pooled buffer wash; 1 M KCl, fractions from the salt elution step (numbers represent fractions); G-Buffer, fractions from the low-ionic-strength elution; 2M urea and 7M urea, washes to remove remaining actin and profilin.

(B) SDS–polyacrylamide gel and anti-actin immunoblot of purified maize pollen actin and RSMA. Lanes 1 and 3 contain 9 μg of purified pollen actin from the 1 M KCl eluate after one cycle of polymerization and depolymerization. Densitometry of the pollen actin sample indicates a purity of >98%. Lanes 2 and 4 contain 10 μg of purified RSMA. Molecular mass markers are given at left in kilodaltons. CB, Coomassie blue–stained SDS–polyacrylamide gel of purified actin samples.

(C) Coomassie blue–stained isoelectric focusing (IEF) gel loaded with (lane 1) 2.5 μg of purified maize pollen actin from the 1 M KCl eluate and (lane 2) 4.5 μg of RSMA. The migration of isoelectric focusing standards is shown at right.

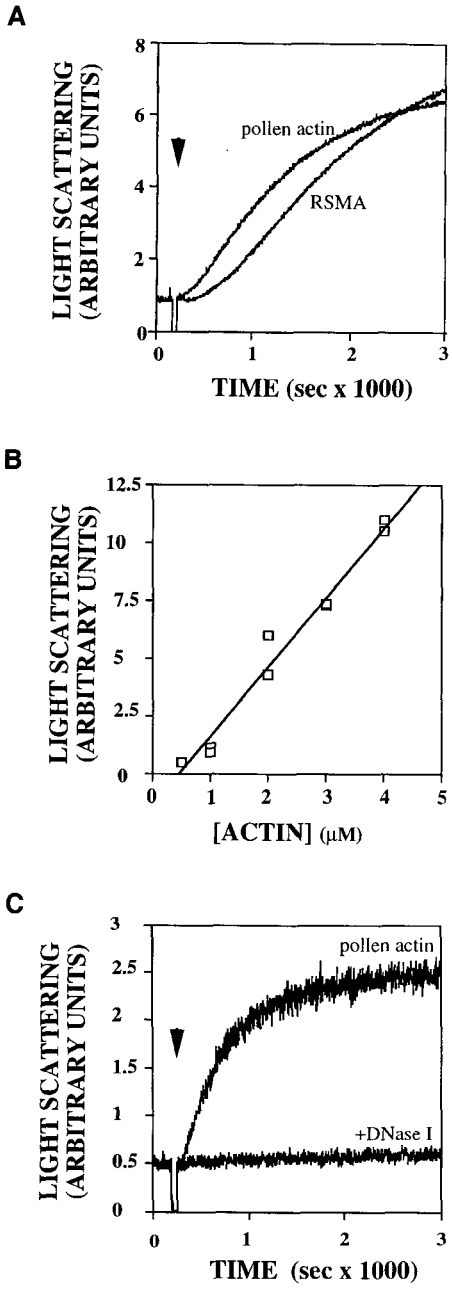

Figure 2. Pollen Actin Polymerization Kinetics and Steady State Polymer Levels.

(A) Time course for actin polymerization measured by 90° light scattering. Samples containing 5 μM G-actin in buffer F without salts were measured for 200 sec before polymerization. Actin polymerization was initiated by the addition of $MgCl_2$ to 5 mM and KCl to 100 mM at the time indicated by the arrowhead, and light scattering was recorded for 3000 sec. Pollen actin is compared with RSMA polymerized under identical conditions.

(B) The critical concentration for actin polymerization determined by measurement of light scattering at steady state. Samples containing 0.5, 1, 2, 3, and 4 μM pollen actin were polymerized for 16 hr after the addition of $MgCl_2$ and KCl, as given above. The amount of polymer at each actin concentration was measured by light scattering, normalized against identical samples without salt, and plotted versus the total actin concentration (open boxes). The intercept with the x-axis of a line of best-fit through these data defines the critical concentration or the amount of actin monomer present at equilibrium. For this experiment, C_c was 0.46 μM, and the average C_c (±SD) for pollen actin was 0.6 ± 0.2 μM (n = 3).

(C) Complete inhibition of pollen actin (7 μM) polymerization in the presence of equimolar amounts of DNase I (+DNase I). Polymerization was initiated by the addition of salts at the time indicated by the arrowhead, and polymer formation was measured by 90° light scattering.

was polymerized at room temperature by the addition of $MgCl_2$ to 5 mM and KCl to 100 mM, the dynamic light scattering profiles demonstrated similarities with those for RSMA, as shown in Figure 2A. A period of rapid polymerization followed a short lag, and assembly reached a plateau or dynamic equilibrium between 2 and 6 hr (data not shown). However, the pollen actin polymerization kinetics differed slightly in several features from those of RSMA (Figure 2A). The lag period was reproducibly shorter, the rate of assembly somewhat faster, and the final extent of polymerization always lower. The amount of F-actin at steady state equilibrium was dependent on the initial actin concentration (Figure 2B). The point at which a line through these data intersects the x-axis is an indication of the amount of unpolymerized monomer present at equilibrium or the critical concentration (C_c). An example from one lot of pollen actin is shown in Figure 2B and has a C_c of 0.46 μM. The average C_c (±SD) for pollen actin is 0.6 ± 0.2 μM (n = 3) and compares with 0.1 ± 0.03 μM (n = 3) for RSMA polymerized under similar conditions (data not shown).

The addition of equimolar amounts of the G-actin binding protein DNase I to the polymerization reaction completely prevented F-actin formation (Figure 2C), demonstrating the formation of a high-affinity 1:1 complex. The rate and extent of pollen actin polymerization were also specifically altered in the presence of maize profilins and Arabidopsis actin depolymerizing factor (data not shown). Pollen F-actin also interacted with the chymotryptic S-1 fragment, or head domain, of myosin, as shown in Figure 3. Examination of the amounts of S-1 in pellets and supernatants after centrifugation revealed that myosin sediments only in the presence of actin and that the interaction is sensitive to ATP. The average percentage of total S-1 (±SD) found in the pellets with pollen or rabbit F-actin was 40.0% ± 1.0% and 38.6% ± 5.7% (n = 3), respectively. The values were reduced to 15.0% ± 1.7% and 9.7% ± 3.5% (n = 3) when an excess of ATP was added to the reaction; they were significantly different ($P < 0.002$) as determined by using the two-tailed t test. These data are consistent with the cross-bridge cycle for myosin; a "rigor" complex forms between the myosin S-1 head and F-actin after nucleotide hydrolysis, and the head disengages from actin when it has bound ATP (Sheterline et al., 1995).

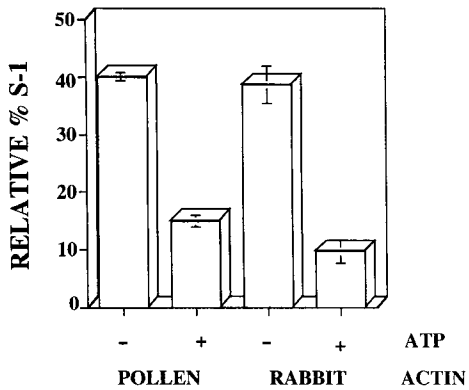

Figure 3. Binding of the Myosin S-1 Fragment to Pollen F-Actin.

The results from three sedimentation experiments in which F-actin was polymerized in the presence of rabbit skeletal muscle myosin S-1 are shown. Equimolar amounts (2 μM each) of RSMA or pollen actin were polymerized in the presence of myosin S-1, and the complex was collected by centrifugation. To test the sensitivity of the interaction to nucleotide, ATP was added to 2 mM just before centrifugation. Myosin S-1 heavy chain was quantified by densitometry of Coomassie blue–stained gels. The values for myosin in the pellet were expressed as a percentage of total myosin added after normalization for the amount of F-actin present and plotted as the average (±SD) of three experiments. Approximately equal amounts (~40%) of myosin S-1 bound to pollen actin and RSMA in the absence (−) of ATP. These levels were reduced in the presence (+) of ATP to an average of 15 and 10% for pollen actin and RSMA, respectively. Values for S-1 sedimenting in the presence of ATP are significantly lower ($P < 0.002$) than those without ATP.

The quality of purified pollen actin was further analyzed ultrastructurally by negative staining of in vitro–polymerized F-actin. Pollen actin and RSMA polymerized under identical conditions were indistinguishable, as shown in Figure 4; both formed long straight polymers with an average diameter of 5 to 7 nm. Qualitatively, the pollen F-actin appears to be somewhat thinner than RMSA (Figure 4B versus Figure 4A), but computer image analysis of scanned images revealed no differences. Pollen actin decorated with myosin S-1 in the absence of ATP was thicker than undecorated actin, with an average diameter of 20 to 27 nm. At higher magnifications, some regions of the decorated polymer showed a characteristic arrowhead appearance (Figure 4C).

Pollen Actin Alleviates the Destructive Effects of High Levels of Profilin in Live Cells

The introduction of excess profilin into live stamen hair cells was shown previously to disrupt cytoarchitecture and to reduce the amount of F-actin (Staiger et al., 1994; Karakesisoglou et al., 1996). This is consistent with a model in which profilin sequesters G-actin from the endogenous monomer pool and prevents filament formation (reviewed in Staiger et al., 1997). Subunits released from the ends of actin filaments would also be bound by profilin and prevented from repolymerizing. If this model is correct, the destructive effects of profilin should be titrated by coinjection with monomeric actin.

The potency of different profilins can be quantified by measuring their ability to displace the nucleus from a central position in Tradescantia stamen hair cells (Gibbon et al., 1997). Disruption of the actin cytoskeleton causes the transvacuolar cytoplasmic strands to become thinner, to lose tension, and ultimately to snap and retract to the peripheral cytoplasm. When a sufficient number of strands are broken, the central nucleus is displaced toward a side wall. For these experiments, we used cells with a reasonably consistent volume, a constant needle load (5 to 10 pL), and identical ABP concentrations (50 μM) for pressure injection. Injected cells were videotaped for 20 min, and the initial nuclear position and the time required to move one nuclear diameter were determined during playback of the video record. At least 20 cells were injected for each treatment, and the results were displayed as a graph of the average time for nuclear displacement (±SE), as shown in Figure 5A.

Injection of buffer alone had little or no effect on nuclear displacement (17.8 ± 1.0 min) compared with a population of uninjected cells (data not shown). Injection of actin-monomer binding proteins such as profilin and DNase I caused a rapid effect on transvacuolar strands, streaming, and nuclear positioning. A needle concentration of 50 μM profilin translated roughly into a 5- to 10-μM addition to the cytoplasm. This amount represents at least a two- to threefold increase over the endogenous pool of profilin in Tradescantia cells, which has been estimated to be 5 μM (Staiger et al., 1994). Because nuclear displacement does not require the complete cessation of streaming or a total disruption of the cytoarchitecture, the concentration used here was lower than the previously reported lowest effective concentration (Staiger et al., 1994). DNase I was most effective at causing nuclear displacement, with an average of 4.8 ± 1.0 min. The recombinant maize profilin ZmPRO4 and human profilin were somewhat less effective at causing nuclear displacement, with average times of 6.8 ± 0.7 min and 6.5 ± 1.0 min, respectively. Many cells were able to recover cytoplasmic streaming, transvacuolar strands, and the central nuclear position by 60 min after these injections (data not shown).

To demonstrate that pollen actin functions in live cells, we tested its ability to prevent the disruptive effects of profilin and DNase I. Figure 5B shows the average nuclear displacement time for a series of injections, including actin alone, equimolar amounts of actin and DNase I, and a 1:1 or 2:1 ratio of actin and profilin. Microinjection of 50 μM actin alone did not cause any perturbation of the cytoarchitecture, streaming, or nuclear position (19.6 ± 0.3 min). When an equimolar mixture of actin and human or maize profilin (50 μM each) was injected, the average nuclear displacement

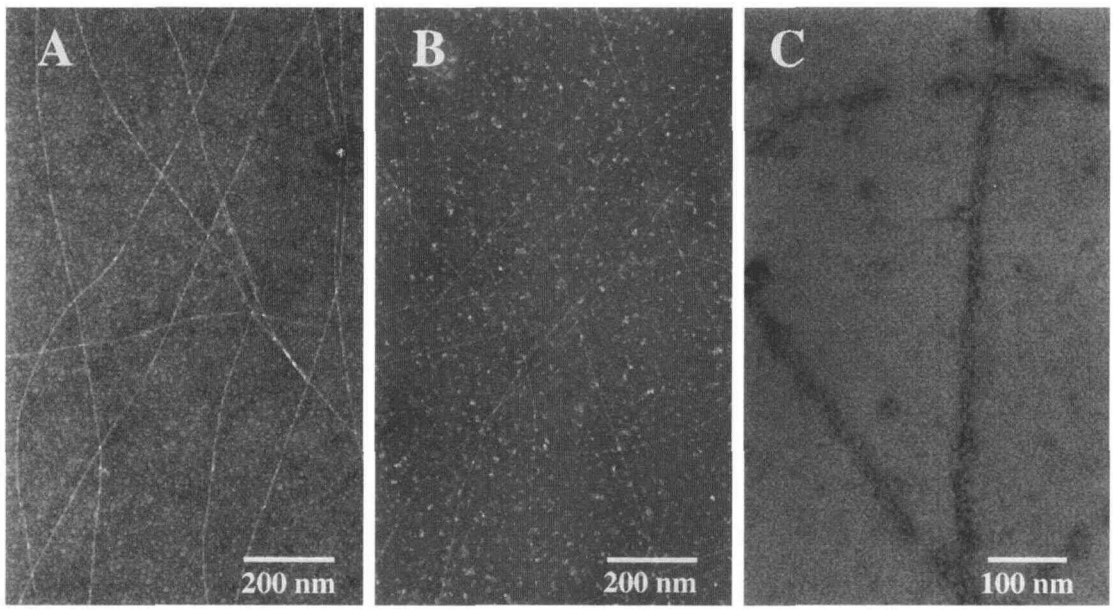

Figure 4. Ultrastructural Examination of Purified F-Actin Decorated with Myosin S-1 Fragment.

(A) RSMA F-actin (7 μM) shows negative staining with phosphotungstic acid.
(B) Maize pollen F-actin (7 μM) stained with phosphotungstic acid.
(C) Pollen actin (14 μM) polymerized in the presence of 14 μM myosin S-1 fragment and stained with uranyl acetate shows a characteristic arrowhead decoration pattern.

times were significantly greater ($P < 0.002$) than those for each profilin alone. Pollen actin plus human profilin had an average displacement time of 16.8 ± 0.9 min, whereas actin plus ZmPRO4 had a time of 11.0 ± 1.0 min. The ability of pollen actin to prevent profilin effects was also dose dependent; at a 2:1 ratio with ZmPRO4, the average nuclear displacement was 15.0 ± 1.1 min. The ability of pollen actin to prevent the destructive effect of DNase I was not quite as dramatic, with an average nuclear displacement time of 7.4 ± 1.3 min, and was not significantly different ($P = 0.11$) from DNase I alone.

Pollen Actin Does Not Perturb Cytoskeletal Organization or Function in Live Cells

Purified pollen actin and RSMA were introduced into the cytoplasm of Tradescantia cells, and F-actin was stained after 15 min with a second injection of fluorescent phalloidin. As shown in Figure 6A, control cells had large bundles of microfilaments in the transvacuolar strands and a fine reticulate meshwork in the peripheral cytoplasm. Increasing the cellular concentration of actin by 5 to 20 μM with RSMA had severe effects on cellular architecture and actin organization. Vertebrate actin polymerized into a massive array of filaments at the site of injection (Figure 6B) and led to the accumulation of cellular organelles (data not shown). The aberrant actin array remained in the cytoplasm for at least 1.5 hr (the limit of our observation period) and correlated with the disruption of streaming and perturbation of cytoarchitecture. Therefore, RSMA did not appear to be compatible with normal cellular function and actin organization in live Tradescantia stamen hair cells. In contrast, injection of pollen actin into the cytoplasm had no apparent negative effects and did not cause the massive polymerization artifact seen with RSMA. After the introduction of 5 to 20 μM plant actin, the normal distribution of F-actin in transvacuolar strands and the cortical cytoplasm was still observed (Figure 6C). Many cells appeared brighter and may have had more microfilaments than did the controls (Figure 6D).

DISCUSSION

A detailed understanding of how plants regulate the spatiotemporal organization of the actin cytoskeleton requires identification of accessory ABPs and a thorough analysis of their physicochemical properties. Higher plants contain multigene families for actin and ABPs, and the biochemical and cell biological characterization of these components has begun in earnest. Most efforts have focused on the motor molecule myosin and the small ABPs profilin and actin depolymerizing factor (reviewed in McCurdy and Williamson, 1991;

Meagher and Williamson, 1994; Asada and Collings, 1997; Staiger et al., 1997). Because of the ease of obtaining large amounts of vertebrate actins, it has become standard practice to analyze actin–plant ABP interactions by reconstitution with heterologous components. For example, plant profilins have been shown to bind rabbit skeletal muscle and bovine cardiac actin isoforms (Giehl et al., 1994; Ruhlandt et al., 1994; Perelroizen et al., 1996). However, it is known that many ABPs interact with nonhomologous sources of actin in a dramatically different fashion (reviewed in Rubenstein, 1990; Hennessey et al., 1993). For example, yeast profilin does not inhibit the polymerization of RSMA but does sequester yeast actin and prevents its polymerization in vitro (Nefsky and Bretscher, 1992). Given the apparent diversity of plant ABP sequences, it will be important to characterize their biochemical properties with physiologically relevant partners. Unfortunately, reports of the isolation and characterization of functional plant actin are limited at present (reviewed in Meagher, 1991; Meagher and Williamson, 1994). To address these problems, we developed a new strategy for the rapid isolation of large quantities of high-quality, polymerization-competent actin from maize pollen.

Pollen is a rich source of cytoskeletal proteins, with estimates for actin ranging from 2 to 20% of total soluble proteins (Andersland et al., 1992; Liu and Yen, 1992; Vidali and Hepler, 1997; this report), and it has served as the starting material for several previous actin purification schemes (Andersland et al., 1992; Liu and Yen, 1992). Our new method represents a significant departure from the earlier methods for plant actin isolation that utilized DNase I affinity chromatography (Kursanov et al., 1983; Kulikova, 1986; McCurdy and Williamson, 1987; Turkina et al., 1987; Villanueva et al., 1990; Andersland et al., 1992; Andersland and Parthasarathy, 1993), combinations of ion exchange and size exclusion chromatography (Metcalf et al., 1980; Vahey and Scordilis, 1980; Vahey et al., 1982; Ghosh and Biswas, 1988; Liu and Yen, 1992), or cycles of polymerization and depolymerization (Ghosh et al., 1987; Ma and Yen, 1989; Liu and Yen, 1992). DNase I forms a high-affinity 1:1 complex with G-actin, and when covalently linked to a chromatography support, it is extremely practical for the isolation of actin from a variety of eukaryotic tissues (Zechel and Weber, 1978). The advantage of this procedure is that formation of the strong DNase I–actin complex (the K_d for RMSA–DNase I is 10^{-9} M) allows a rapid, single-step isolation of actin from crude extracts. A major drawback, however, is that to elute actin from DNase I, both

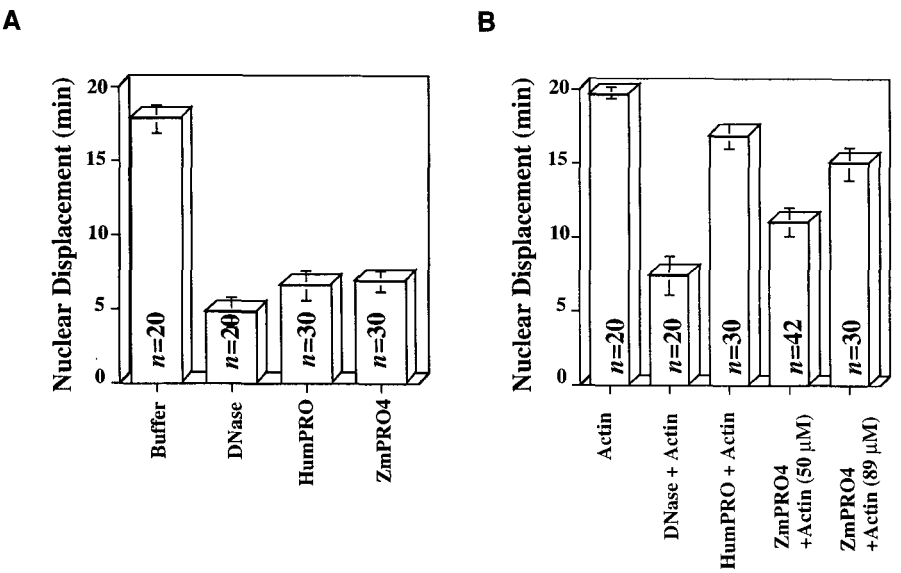

Figure 5. Pollen Actin Prevents the Nuclear Displacement Caused by Injection of Profilin into Live Cells.

(A) Profilin and DNase I are potent disruptors of cytoarchitecture. Stamen hair cells of *T. virginiana* were pressure injected with 50 μM needle concentration of each protein solution. Average nuclear displacement times for at least 20 successful injections were measured for buffer alone, DNase I, recombinant human profilin (HumPRO), and recombinant maize profilin (ZmPRO4). The average nuclear displacement times (±SE) were 17.8 ± 1.0, 4.8 ± 1.0, 6.5 ± 1.0, and 6.8 ± 0.7 min, respectively.

(B) Coinjection of pollen actin alleviated the disruptive effects caused by profilin. Pollen actin alone at 50 μM needle concentration had no effect on cytoarchitecture and gave an average nuclear displacement time of 19.6 ± 0.3 min. When coinjected at a 1:1 stoichiometry with profilin or DNase I, pollen actin increased the average displacement time: DNase I plus actin of 7.4 ± 1.3 min; human profilin plus actin of 16.8 ± 0.8 min; and ZmPRO4 plus actin of 11.0 ± 1.0 min. The preventive effect of pollen actin is dose dependent; a 2:1 stoichiometry of actin–ZmPRO4 has a nuclear displacement time of 15.0 ± 1.1 min.

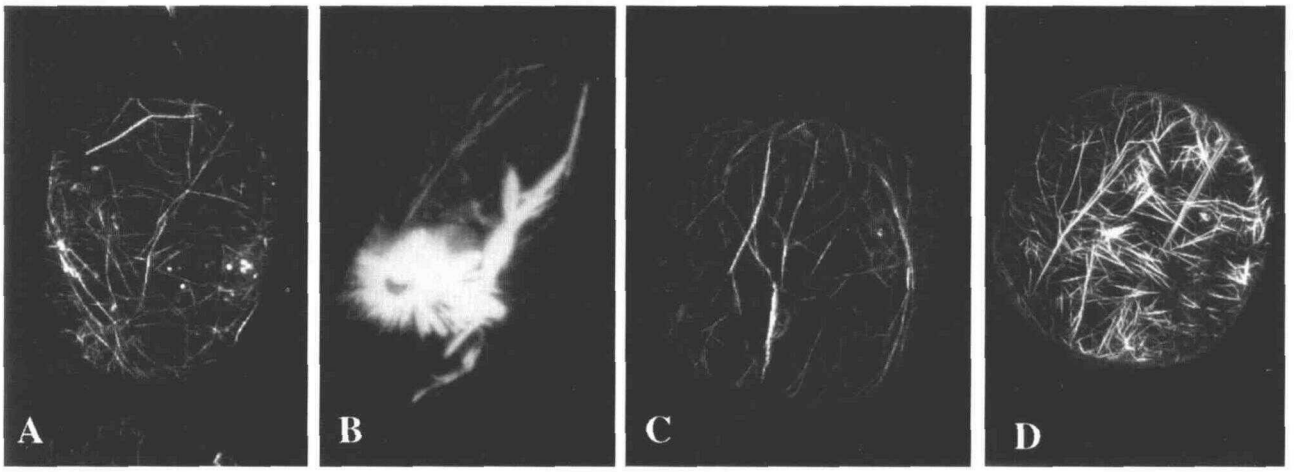

Figure 6. Injection of Pollen Actin into Live Cells Does Not Alter F-Actin Organization.

(A) A *T. blossfeldiana* stamen hair cell injected with fluorescent phalloidin shows the endogenous microfilament array.
(B) A stamen hair cell injected with 67 μM (needle concentration) RSMA has an aberrant microfilament array.
(C) Injection of 67 μM (needle concentration) maize pollen actin and subsequent F-actin labeling shows a normal distribution of microfilaments in this stamen hair cell.
(D) An example of 67 μM pollen actin injection that resulted in a noticeably brighter actin array.

proteins must be partially denatured by chaotropes, such as formamide or urea. In all cases in which polymerization of plant actin purified by the DNase method has been reported, phalloidin or poly-L-lysine was required to drive polymerization or to stabilize F-actin (Turkina et al., 1987; Andersland et al., 1992; Andersland and Parthasarathy, 1993). We faced similar difficulties with DNase I–isolated maize pollen actin (C.J. Staiger, unpublished data) and found that plant actin isolated by profilin chromatography does not tolerate 1 M KI or 2 M urea and does not remain assembly competent.

Our new method uses another G-actin binding protein, profilin, for the indirect isolation of native actin through immobilization of the profilin–actin complex on a PLP–Sepharose column. A similar strategy was used by Grolig and co-workers to reconstitute the profilin–actin complex in vitro and to isolate small amounts of actin from the green alga *Chara corallina* (Ruhlandt et al., 1994). The general outline of our procedure includes preparation of a soluble protein extract from frozen maize pollen, the addition of recombinant profilin, affinity chromatography on PLP–Sepharose, high-ionic-strength elution of actin, and a cycle of assembly and disassembly. Two key parameters for the successful isolation of maize pollen actin are the addition of excess profilin to pollen extracts and the choice of vertebrate profilin. The first step may serve to depolymerize endogenous F-actin in the pollen extracts and thereby enhance yields of G-actin. The choice of vertebrate profilin was motivated by preliminary studies in which human profilin bound substantially more pollen actin than did several recombinant maize pollen profilins. We have recently established that human profilin has a significantly higher affinity for purified pollen G-actin under low-ionic-strength conditions (Gibbon et al., 1997). This is also consistent with the observation that plant profilins have a lower affinity for vertebrate actin isoforms than do bovine spleen or thymus profilin (Giehl et al., 1994; Perelroizen et al., 1996). Although endogenous profilin may be present in equimolar amounts with actin in pollen extracts (Vidali and Hepler, 1997), the low affinity of the interaction may prevent the isolation of large amounts of profilin–actin complex (see Ruhlandt et al., 1994).

As with DNase I affinity chromatography, the ability to separate actin rapidly from the crude cytoplasmic extract may minimize proteolysis. We also used a buffer that was developed for the isolation of a high-affinity profilin–actin complex from vertebrate cells (Katakami et al., 1992). The basis for the efficacy of this buffer is poorly understood, but the inclusion of phosphatase inhibitors (NaPPi and NaF) has been suggested to function in maintaining the phosphorylation of one of the components of the profilin–actin complex or a minor accessory factor necessary for stabilization (Katakami et al., 1992). Alternatively, as suggested by Andersland et al. (1992) from studies of DNase I–actin isolation, it may be necessary to inhibit endogenous ATPase activity in plant extracts to maintain the high levels of ATP required for actin–ABP interactions.

This new procedure provides a source of native plant actin that is high in quality, readily polymerizable, pure, and abundant. The average yield of 6 mg of actin from 10 g of pollen is at least threefold higher than the yield obtained using a previous method for isolating actin from maize (Liu and Yen,

1992). Liu and Yen (1992) developed a protocol involving the preparation of a pollen acetone powder, low-ionic-strength extraction, ammonium sulfate precipitation, anion exchange chromatography, polymerization and depolymerization, and size exclusion chromatography. Their procedure provides up to 2 mg of actin from 10 g of pollen at an apparent purity of 92% (Liu and Yen, 1992). Our new strategy generates polymerizable actin that is >98% pure in less than half of the time.

These high yields enabled us to examine the physicochemical properties of native plant actin. We have shown that pollen actin under physiological ionic conditions polymerizes with kinetics similar in quality to those of RSMA. After the addition of salts to a solution of G-actin, a short initial lag period is followed by rapid assembly. The lag, typically considered to be a nucleation phase for seed formation (Sheterline et al., 1995), is reproducibly shorter for pollen actin than for RSMA. One remote possibility is that the pollen actin preparations contain an accessory protein that can seed the polymerization reaction. However, such a factor would have to be present in extremely minor amounts, because we did not detect contaminants on overloaded SDS–polyacrylamide gels stained with Coomassie blue. The simplest explanation for the shorter nucleation phase is that the pollen actin has already undergone one cycle of assembly and disassembly and thus may contain short oligomers. Future studies that include a size exclusion chromatograpy step should address this point.

During the elongation phase, native pollen actin polymerizes at a rate similar to or even slightly faster than the RSMA rate. This differs from the assembly kinetics reported by Yen et al. (1995), who observed that pollen actin assembles at dramatically slower rates than does RSMA. At equilibrium, the amount of F-actin formed is dependent on the initial concentration of actin. The amount of actin that remains unpolymerized is known as the critical concentration for assembly and, for muscle α-actin, has a value of $\sim$0.1 μM (Sheterline et al., 1995). Native pollen actin has a C_c of 0.6 μM. These differences could reflect species-specific differences in the rate of monomer exchange at the ends of the filaments. Alternatively, a small amount of nonfunctional actin may be present in the pollen actin samples. A third possibility is that our measured critical concentration reflects assembly kinetics at only one end of the plant actin polymer. A difference between the critical concentrations at the opposite ends of each actin filament is known for RSMA; the fast-growing or barbed end of actin has a C_c of 0.1 μM, and the slow-growing or pointed end has a C_c of 1 μM (Sheterline et al., 1995). The presence of a barbed-end capping factor could prevent addition at the fast-growing ends of many filaments and lead to an apparent critical concentration that reflects pointed-end assembly (Casella et al., 1995). Because rate constants for assembly also differ at the two ends of F-actin (Pollard, 1986), it is predicted that the elongation rate would be reduced in the presence of a barbed-end capping factor. This was not observed during pollen actin polymerization.

Purified pollen actin interacts with a number of ABPs in vitro. One important criterion for demonstrating the authenticity of purified actin is the ability of the polymer to bind myosin and proteolytic fragments of the head domain (HMM and S-1). Pollen actin polymerizes into 5- to 7-nm filaments that can be decorated with rabbit skeletal myosin S-1 fragments. Moreover, by using cosedimentation analyses, we showed that this interaction is nucleotide dependent; S-1 is largely released from F-actin in the presence of excess ATP. In addition to myosin and vertebrate profilin, purified pollen actin also associates with DNase I, as evidenced by the complete inhibition of actin polymerization in the presence of equimolar amounts. The ability to purify large quantities of actin has also enabled us to examine polymerization kinetics, demonstrate association with polymer or monomer, and measure dissociation constants for the plant ABPs, profilin and actin depolymerizing factor. The details of these studies will be published elsewhere (Gibbon et al., 1997; L.E. Zonia, B.C. Gibbon, P.J. Hussey, and C.J. Staiger, manuscript in preparation) but provide supporting evidence for the functionality of the pollen actin.

Ultimately, it will be important to investigate the functional properties of plant actin and ABPs in the living cell in which signaling molecules and the full battery of accessory factors modulate actin organization in a complex fashion. We have used Tradescantia stamen hair cells (reviewed in Hepler et al., 1993) to develop a model system for analyzing the effects of various perturbations on actin organization. We demonstrated previously that increasing the cellular concentration of G-actin binding proteins, by injection of pollen profilin or DNase I, led to a dose-dependent reduction in F-actin (Staiger et al., 1994; Karakesisoglou et al., 1996). This is consistent with a sequestering model in which binding of profilin (or DNase I) to monomeric actin promotes actin depolymerization (reviewed in Staiger et al., 1997). Coinjection of monomeric actin and profilin should thus titrate the sequestering function of profilin.

To quantify the effects of profilin and DNase I, we developed a method to monitor the actin cytoskeletal structure that maintains nuclei in a centralized position. Using this nuclear displacement assay, we determined that injection of a 1:1 or 2:1 ratio of actin to profilin results in less disruption to the cyto-architecture than does human or plant profilin alone. Moreover, we have examined the cytological effects of introducing excess monomeric actin into the plant cell cytoplasm. RSMA is not compatible with the endogenous array in Tradescantia stamen cells (for additional observations, see Hepler et al., 1993) and forms an aberrant array of polymeric actin at the site of injection. On the other hand, plant actin causes no apparent disruption of F-actin organization or cytoarchitecture when injected at identical concentrations. Many cells with normal arrays appear brighter than controls. These results provide evidence that pollen actin is fully functional in the complex cellular environment. Further proof for this will be sought by generating fluorescent analogs of actin and introducing them into the cytoplasm of living cells.

Prospects for Future Investigation

The methods reported here should provide a convenient source of plant actin for biochemical and cell biological analyses to members of any laboratory interested in pursuing cytoskeleton research. The large quantities that can be rapidly obtained will greatly facilitate future studies designed to reconstitute physiologically relevant interactions between plant actin and plant ABPs. Furthermore, the ability of pollen actin to function in the living plant cell raises the possibility of performing measurements of actin dynamics in vivo with the powerful techniques of fluorescent analog cytochemistry and digital image analysis.

METHODS

Materials

Pollen was collected from maize (*Zea mays*) plants grown in a summer field plot (Purdue Agronomy Research Farm, West Lafayette, IN) during the months of July and August and stored at −75°C. Poly-L-proline (PLP; 10 to 30 kD), phenylmethylsulfonyl fluoride (PMSF), aprotinin, leupeptin, pepstatin A, benzamidine, phenanthroline, and electrophoretically pure DNase I (DN-EP) were purchased from Sigma. Na_2-ATP and DTT were purchased from U.S. Biochemical. PLP was conjugated to CNBr-activated Sepharose 4B (Pharmacia Biotech Inc.), according to the methods of Rozycki et al. (1991). Recombinant human profilin I was overexpressed in *Escherichia coli*, using a full-length cDNA in the expression vector pMW172 (kindly provided by S. Almo, Albert Einstein University, The Bronx, NY; Fedorov et al., 1994). The maize profilin ZmPRO4 (L.E. Zonia, B.C. Gibbon, P.J. Hussey, and C.J. Staiger, manuscript in preparation) was expressed using the vector pET-3a (Novagen, Inc., Madison, WI), according to the strategy used for the pollen profilins (Karakesisoglou et al., 1996). Profilins were purified using PLP affinity chromatography, as described previously (Karakesisoglou et al., 1996). Rabbit skeletal muscle actin (RSMA) was prepared by the methods of Pardee and Spudich (1982), with the modifications suggested by MacLean-Fletcher and Pollard (1980). Protein concentrations were determined with the Bradford reagent (Bio-Rad), using BSA as a standard.

Solutions

The protein inhibitor mixture (PI cocktail) was composed of 1.6 mg/mL benzamidine, 0.1 mg/mL phenanthroline, and 1 mg/mL each of aprotinin, leupeptin, and pepstatin A suspended in ethanol and stored at −20°C. A 100 mM PMSF stock solution was prepared in isopropanol. Buffer A was modified from Katakami et al. (1992) and contained 10 mM Tris, pH 8.5, 0.5 mM $CaCl_2$, 0.01% NaN_3, 50 mM NaF, 30 mM NaPPi, 0.4 mM ATP, 0.5 mM DTT, 0.5 mM PMSF, and 1/200 PI cocktail. Buffer B included 5 mM Tris, pH 7.5, 0.2 mM $CaCl_2$, 0.01% NaN_3, 50 mM NaF, 30 mM NaPPi, 0.4 mM ATP, and 0.5 mM DTT. Buffer G was composed of 5 mM Tris, pH 7.0 or 8.0 as noted, 0.2 mM $CaCl_2$, 0.01% NaN_3, 0.2 mM ATP, and 0.5 mM DTT. Buffer F contained 5 mM Hepes, pH 7.0, 5 mM $MgCl_2$, 0.2 mM ATP, and 100 mM KCl. Buffer I contained 20 mM Tris, pH 7.5, 0.2 mM DTT, and 150 mM KCl.

Isolation and Purification of Pollen Actin and Actin–Profilin Complex

A 10-g sample of frozen maize pollen was ground in a mortar with 20 mL of ice-cold buffer A for 20 min. The homogenate was supplemented with an additional 30 mL of buffer A and then sonicated (model 300 Sonic Dismembranator; Fisher Scientific Co., Pittsburgh, PA) using 5 × 20 sec bursts. All subsequent steps, except where noted, were performed at 0 to 4°C. The extract was centrifuged at 30,000*g* for 20 min, and the supernatant was removed, avoiding the lipid-containing layer. Further clarification of this supernatant was performed at 46,000*g* for 30 min. The clarified supernatant was adjusted to pH 7.5, using 0.5 M NaOH, supplemented with 20 mg of recombinant human profilin I, 1/200 PI cocktail, 0.5 mM PMSF, and 0.4 mM ATP, and then centrifuged at 100,000*g* for 1 hr. The supernatant was applied to a PLP–Sepharose affinity column (15 mL) pre-equilibrated with buffer B at a flow rate of <1 mL/min. After the sample was loaded, the column was washed with 3 column volumes of buffer B. Actin was eluted with 3 bed volumes of 1 M KCl in buffer G, pH 8.0, and collected as 2-mL fractions, followed by the elution of a profilin–actin complex with buffer G, pH 8.0, alone. The remaining actin and profilin were eluted from the column by washes of 2 and 7 M urea in buffer I.

The fractions containing >0.2 mg/mL actin or profilin–actin were pooled separately and dialyzed twice against buffer G, pH 8.0, and once against buffer G, pH 7.0, over 12 to 16 hr. Dialyzed fractions were clarified by centrifugation at 100,000*g* for 1 to 2 hr. Actin was polymerized by adding $MgCl_2$ to 5 mM and KCl to 100 mM and incubating at room temperature for 2 hr and then at 4°C overnight. Filamentous actin (F-actin) was collected by centrifugation at 100,000*g* for 3 hr. The pellet was resuspended with buffer G, pH 8.0, and depolymerized by dialysis against three changes of buffer G, pH 8.0, over 3 days. G-actin was recovered after centrifugation of the dialyzed sample to remove undepolymerized actin filaments. For all biochemical experiments, we used 1 M KCl-eluted actin that was freshly cycled or stored for 1 to 2 days at 4°C as G-actin. Pollen G-actin also could be frozen in small aliquots (10 to 100 μL) in liquid nitrogen and stored at −75°C for periods of several months with moderate loss of activity. Previously frozen pollen actin was used for microinjection experiments (see below).

Polymerization Kinetics and Determination of Critical Concentration for Assembly

Actin polymerization and steady state polymer levels were measured by 90° light scattering, as described by Cooper and Pollard (1982). Dynamic polymerization was monitored over a 50-min period with a spectrophotometer (model 8000; SLM Instruments Inc., Urbana, IL) set for excitation and emission wavelengths of 450 nm. For the critical concentration (C_c) determination, quadruplicate samples containing 0.5, 1, 2, 3, and 4 μM G-actin in 1.6 mL of buffer F, pH 7.0, without salt, were prepared. At time zero, salts were added to a final concentration of 5 mM $MgCl_2$ and 100 mM KCl to half of the samples, and polymerization was allowed to proceed for 16 hr. Light scattering measurements for polymerized actin were normalized against the readings from same concentration G-actin controls (no salt added) taken at 16 hr.

Sedimentation of the Myosin S-1 Fragment with Pollen F-Actin

Skeletal muscle myosin was purified from the back and hind muscles of a New Zealand white rabbit, using the method of Pollard (1982),

and stored as an ammonium sulfate precipitate at 4°C. The single-headed myosin S-1 fragment was prepared by chymotryptic digestion, according to Weeds and Taylor (1975), followed by purification on DEAE–cellulose. To demonstrate specific interaction with F-actin, equimolar amounts (2 μM each) of the chymotryptic S-1 fragment and pollen or rabbit skeletal muscle F-actin were added to buffer F for a final volume of 100 μL and allowed to equilibrate at 4°C for 2 to 3 hr. Polymeric actin and bound myosin were collected by centrifugation at 300,000*g* for 30 min. Supernatants were removed and prepared for gel electrophoresis by the addition of 25 μL of 5× protein sample buffer (Laemmli, 1970). Individual pellets were resuspended in 125 μL of 2× protein sample buffer. Equivalent volumes of each pellet and supernatant sample were separated by SDS-PAGE (see below). The amount of S-1 heavy chain in the pellets was determined by densitometry (personal densitometer; Molecular Dynamics, Inc., Sunnyvale, CA) of Coomassie Brilliant Blue R 250–stained (Sigma) gels and expressed as a percentage of the total amount of myosin added to the reaction. Myosin S-1 did not sediment in the absence of F-actin under these conditions. These values were normalized for the amount of actin present in the pellet, because more F-actin was typically present in pellets of vertebrate actin versus pollen actin.

Electron Microscopy of in Vitro–Polymerized F-Actin

Samples containing 7 μM actin filaments in buffer F were applied to Formvar plus carbon-coated grids and negatively stained with 1% phosphotungstic acid, pH 7.2, or 2% uranyl acetate. The specimens were visualized in a microscope (model EM400; Philips Electronic Instruments, Inc., Mahwah, NJ) at an accelerating voltage of 80 kV. Actin filaments were decorated by the addition of 14 μM myosin S-1 fragment to 14 μM actin in buffer F. After samples were incubated at room temperature for 30 min, the resulting complexes were deposited on grids and stained as given above.

Electrophoresis and Immunoblotting

Samples were electrophoresed on 15% polyacrylamide gels and then stained with Coomassie blue or transferred to nitrocellulose (BA-83; Schleicher & Schuell). Protein immunoblotting was performed as described previously (Xu et al., 1992). Actin was detected using a mouse monoclonal antibody raised against chicken gizzard actin (Lessard, 1988; a kind gift of J. Lessard, Children's Hospital, Cincinnati, OH) as the primary antibody and horseradish peroxidase–conjugated anti–mouse IgG (Sigma) as the secondary antibody. The antigen–antibody complex was detected using 0.025% (v/v) hydrogen peroxide with 0.5 mg/mL 4-chloro-1-naphthol as the substrate.

Isoelectric focusing gels were composed of 9.2 M urea, 5% acrylamide (19:1 acrylamide-bis), 2% Triton X-100, 1.6% 4/6 Biolyte ampholytes (Bio-Rad), and 0.6% 3/10 Biolyte ampholytes. Upper and lower chamber buffers were 100 mM NaOH and 10 mM H_3PO_4, respectively. Samples were prepared by adding 3 to 5 μg of protein to the sample buffer (9.5 M urea, 5% β-mercaptoethanol, 2% Triton X-100, 1.6% 4/6 Biolyte ampholyte, and 0.4% 3/10 Biolyte ampholyte). Samples were loaded into wells, covered with overlay buffer (9 M urea, 0.8% 4/6 Biolyte ampholyte, and 0.2% 3/10 Biolyte ampholyte), and electrophoresed with increasing voltage steps (100, 300, and 600 V) for a total of 1500 V/hr. Heating was minimized by frequent exchanges of the upper chamber buffer. Isoelectric points were calculated by plotting retardation factor versus pI of known standard proteins (Sigma).

Microinjection of Stamen Hair Cells

Stamen hairs were collected from open flowers of Tradescantia (*T. virginiana* or *T. blossfeldiana*) and immobilized for microinjection, as described previously (Staiger et al., 1994; Karakesisoglou et al., 1996). Individual cells located four to six cells distal from the apical tip were used for all microinjections. Only cells with a nucleus positioned in the middle of the vacuole and supported by transvacuolar strands were injected. The ability of purified pollen actin to prevent the destructive effects of profilin on live plant cells was examined by microinjection of recombinant human or ZmPRO4 and profilin–actin complexes. Recombinant profilins and DNase I were concentrated, and the buffer was exchanged with 5 mM Tris, pH 7.5, and 0.2 mM DTT, using Centrex-2 10-kD molecular weight cut-off ultrafiltration devices (Schleicher & Schuell). Pollen actin in buffer G was exchanged with actin microinjection buffer (2 mM Tris–acetate, pH 7.5, 0.1 mM DTT, 0.2 mM ATP, and 50 mM $MgCl_2$). Actin was frozen in 10-μL aliquots and stored at −75°C. All solutions were clarified by centrifugation at 12,000*g* for 30 min before microinjection.

Actin was injected alone or was supplemented with a small volume of purified profilin to yield an equimolar ratio of each protein. Microneedles pulled from borosilicate glass capillaries (GC100T-10; Warner Instruments Corp., Hamden, CT) were front-loaded to a measured distance (approximate volume of 5 to 10 pL) with 50 μM profilin, DNase I, or profilin–actin solutions. The volume of injected solution typically resulted in an increase of 10 to 20% of the cytoplasmic volume. Cell behavior after injection was monitored using a monochrome single-chip CCD camera (model JE-7442; Javelin Electronics, Torrance, CA) and recorded onto VHS tape. The ability of profilin to cause displacement of the nucleus from a central position was measured during replay of the video footage. At time zero, when the entire needle contents had entered the cell, the position of the nucleus was traced on a sheet of cellulose acetate attached to the video monitor. The measured nuclear displacement time was the period required for a particular treatment to cause the nucleus to move completely outside the original perimeter. If the nucleus failed to move outside the original perimeter during the observation period, a value of 20 min was recorded. At least 20 to 30 cells were examined for each treatment, and controls included injection with buffer alone.

F-actin in live stamen hair cells was stained by microinjection of fluorescent phalloidin (FITC–phalloidin [Sigma] or rhodamine–phalloidin [Molecular Probes, Inc., Eugene, OR]), and images were acquired with a confocal laser scanning microscope (model MRC 1024; Bio-Rad). Stock solutions of fluorescent phalloidin in methanol were air dried and resuspended in microinjection buffer to a final concentration of 30 μM. Needles were front-loaded as given above, cells were loaded by pressure injection, and the needle was removed after 4 to 5 min. A coverslip was applied, the position of the injected cell was recorded with an England Finder (Graticules Ltd., Tonbridge, UK), and the slide was transferred to the stage of a Nikon (Melville, NY) optiphot that served as the base for the confocal laser scanning microscope. Cells were imaged through a 60X Nikon Planapo objective (1.4 NA), using illumination from the 488 or 568 line of the Kr/Ar laser. Data from the upper half of a transverse section of each cell were acquired by collecting Kalman-filtered scans at individual steps of 1.3 μm each. Cells were reconstructed as projections by using the LaserSharp software package (Bio-Rad) and prepared for presentation by using the National Institutes of Health Image software (version

1.54). Electronic images were printed using a Tektronix (Beaverton, OR) *Phaser II SDX dye sublimation printer.*

ACKNOWLEDGMENTS

This research was supported by grants from the U.S. Department of Agriculture–National Research Initiative Competitive Grants Program (No. 94-37304-1179) and the Purdue Research Foundation to C.J.S. and by a National Science Foundation (NSF) Plant Genetics Traineeship (No. 9355012 GEF) to B.C.G. The confocal microscopy facility was supported in part by a grant from the NSF (No. BIR 9512962). We thank members of the Staiger, David Asai, and Joann Otto laboratories for helpful advice and Dr. Laura Zonia for critical review of the manuscript. Portions of this work have been published in abstract form (H. Ren, W. Grubb, S.L. Ashworth, B. Gibbon, and C.J. Staiger [1996]. Mol. Biol. Cell **7S,** 375a, 2177).

Received March 26, 1997; accepted June 5, 1997.

REFERENCES

Andersland, J.M., and Parthasarathy, M.V. (1993). Conditions affecting depolymerization of actin in plant homogenates. J. Cell Sci. **104,** 1273–1279.

Andersland, J.M., Jagendorf, A.T., and Parthasarathy, M.V. (1992). The isolation of actin from pea roots by DNase I affinity chromatography. Plant Physiol. **100,** 1716–1723.

Asada, T., and Collings, D. (1997). Molecular motors in higher plants. Trends Plant Sci. **2,** 29–37.

Carlier, M.-F., Laurent, V., Santolini, J., Melki, R., Didry, D., Xia, G.-X., Hong, Y., Chua, N.-H., and Pantaloni, D. (1997). Actin depolymerizing factor (ADF/cofilin) enhances the rate of filament turnover: Implication in actin-based motility. J. Cell Biol. **136,** 1307–1322.

Casella, J.F., Barron-Casella, E.A., and Torres, M.A. (1995). Quantitation of Cap Z in conventional actin preparations and methods for further purification of actin. Cell Motil. Cytoskeleton **30,** 164–170.

Chen, X., Sullivan, D.S., and Huffaker, T.C. (1994). Two yeast genes with similarity to TCP-1 are required for microtubule and actin function in vivo. Proc. Natl. Acad. Sci. USA **91,** 9111–9115.

Cooper, J.A., and Pollard, T.D. (1982). Methods to measure actin polymerization. Methods Enzymol. **85,** 182–210.

Fedorov, A.A., Pollard, T.D., and Almo, S.C. (1994). Purification, characterization and crystallization of human platelet profilin expressed in *Escherichia coli*. J. Mol. Biol. **241,** 480–482.

Ghosh, G., and Biswas, S. (1988). An actin of higher plant: Purification and characterization. Plant Physiol. Biochem. **15,** 153–160.

Ghosh, G., Mukherjee, J., and Biswas, S. (1987). Actin-like protein from *Mimosa pudica* L. Indian J. Biochem. Biophys. **24,** 336–339.

Gibbon, B.C., Ren, H., and Staiger, C.J. (1997). Characterization of maize pollen profilins in vitro and in live cells. Biochem. J., in press.

Giehl, K., Valenta, R., Rothkegel, M., Ronsiek, M., Mannherz, H.-G., and Jockusch, B.M. (1994). Interaction of plant profilin with mammalian actin. Eur. J. Biochem. **226,** 681–689.

Hennessey, E.S., Drummond, D.R., and Sparrow, J.C. (1993). Molecular genetics of actin function. Biochem. J. **282,** 657–671.

Hepler, P.K., Cleary, A.L., Gunning, B.E.S., Wadsworth, P., Wasteneys, G.O., and Zhang, D.H. (1993). Cytoskeletal dynamics in living plant cells. Cell Biol. Int. **17,** 127–142.

Karakesisoglou, I., Schleicher, M., Gibbon, B.C., and Staiger, C.J. (1996). Plant profilins rescue the aberrant phenotype of profilin-deficient *Dictyostelium* cells. Cell Motil. Cytoskeleton **34,** 36–47.

Katakami, Y., Katakami, N., Janmey, P.A., Hartwig, J.H., and Stossel, T.P. (1992). Isolation of the phosphatidylinositol 4-monophosphate dissociable high-affinity profilin–actin complex. Biochim. Biophys. Acta **1122,** 123–135.

Kim, E., Miller, C.J., and Reisler, E. (1996). Polymerization and in vitro motility properties of yeast actin: A comparison with rabbit skeletal α-actin. Biochemistry **35,** 16566–16572.

Kulikova, A.L. (1986). Quantity and forms of actin in conducting tissues of *Heracleum sosnowskyi*. Russian J. Plant Physiol. **33,** 481–487.

Kursanov, A.L., Kulikova, A.L., and Turkina, M.V. (1983). Actin-like protein from the phloem of *Heracleum sosnowskyi*. Physiol. Vég. **21,** 353–360.

Laemmli, U.K. (1970). Cleavage of structural proteins during the assembly of the head of bacteriophage T4. Nature **227,** 680–684.

Lessard, J.L. (1988). Two monoclonal antibodies to actin: One muscle selective and one generally reactive. Cell Motil. Cytoskeleton **10,** 349–362.

Liu, X., and Yen, L.-F. (1992). Purification and characterization of actin from maize pollen. Plant Physiol. **99,** 1151–1155.

Lopez, I., Anthony, R.G., Maciver, S.K., Jiang, C.-J., Khan, S., Weeds, A.G., and Hussey, P.J. (1996). Pollen specific expression of maize genes encoding actin depolymerizing factor–like proteins. Proc. Natl. Acad. Sci. USA **93,** 7415–7420.

Ma, Y.-Z., and Yen, L.-F. (1989). Actin and myosin in pea tendrils. Plant Physiol. **89,** 586–589.

MacLean-Fletcher, S., and Pollard, T.D. (1980). Identification of a factor in conventional muscle actin preparations which inhibits actin filament self-association. Biochem. Biophys. Res. Commun. **96,** 18–27.

McCurdy, D.W., and Williamson, R.E. (1987). An actin-related protein inside pea chloroplasts. J. Cell Sci. **87,** 449–456.

McCurdy, D.W., and Williamson, R.E. (1991). Actin and actin-associated proteins. In The Cytoskeletal Basis of Plant Growth and Form, C.W. Lloyd, ed (London: Academic Press), pp. 3–14.

Meagher, R.B. (1991). Divergence and differential expression of actin gene families in higher plants. Int. Rev. Cytol. **125,** 139–163.

Meagher, R.B., and McLean, B.G. (1990). Diversity of plant actins. Cell Motil. Cytoskeleton **16,** 164–166.

Meagher, R.B., and Williamson, R.E. (1994). The plant cytoskeleton. In *Arabidopsis*, E. Meyerowitz and C. Somerville, eds (Cold Spring Harbor, NY: Cold Spring Harbor Laboratory Press), pp. 1049–1084.

Metcalf III, T.N., Szabo, L.J., Schubert, K.R., and Wang, J.L. (1980). Immunocytochemical identification of an actin-like protein from soybean seedlings. Nature **285,** 171–172.

Nefsky, B., and Bretscher, A. (1992). Yeast actin is relatively well behaved. Eur. J. Biochem. **206,** 949–955.

Pardee, J.D., and Spudich, J.A. (1982). Purification of muscle actin. Methods Cell Biol. **24,** 271–289.

Perelroizen, I., Didry, D., Christensen, H., Chua, N.-H., and Carlier, M.-F. (1996). Role of nucleotide exchange and hydrolysis in the function of profilin in actin assembly. J. Biol. Chem. **271,** 12302–12309.

Pollard, T.D. (1982). Myosin purification and characterization. Methods Cell Biol. **24,** 333–371.

Pollard, T.D. (1986). Rate constants for the reactions of ATP- and ADP-actin with the ends of actin filaments. J. Cell Biol. **103,** 2747–2754.

Rozycki, M., Schutt, C.E., and Lindberg, U. (1991). Affinity chromatography-based purification of profilin:actin. Methods Enzymol. **196,** 100–118.

Rubenstein, P.A. (1990). The functional importance of multiple actin isoforms. Bioessays **12,** 309–315.

Ruhlandt, G., Lange, U., and Grolig, F. (1994). Profilins purified from higher plants bind to actin from cardiac muscle and to actin from a green alga. Plant Cell Physiol. **35,** 849–854.

Sheterline, P., Clayton, J., and Sparrow, J.C. (1995). Actin. Protein Profile **2,** 1–103.

Staiger, C.J., and Lloyd, C.W. (1991). The plant cytoskeleton. Curr. Opin. Cell Biol. **3,** 33–42.

Staiger, C.J., Yuan, M., Valenta, R., Shaw, P.J., Warn, R., and Lloyd, C.W. (1994). Microinjected profilin affects cytoplasmic streaming in plant cells by rapidly depolymerizing actin microfilaments. Curr. Biol. **4,** 215–219.

Staiger, C.J., Gibbon, B.C., Kovar, D.R., and Zonia, L.E. (1997). Profilin and actin-depolymerizing factor: Modulators of actin organization in plants. Trends Plant Sci. **2,** 275–281.

Turkina, M.V., Kulikova, A.L., Sokolov, O.I., Bogatyrev, V.A., and Kursanov, A.L. (1987). Actin and myosin filaments from the conducting tissues of *Heracleum sosnowskyi*. Plant Physiol. Biochem. **25,** 689–696.

Vahey, M., and Scordilis, S.P. (1980). Contractile proteins from tomato. Can. J. Bot. **58,** 797–801.

Vahey, M., Titus, M., Trautwein, R., and Scordilis, S. (1982). Tomato actin and myosin: Contractile proteins from a higher land plant. Cell Motil. **2,** 131–147.

Vidali, L., and Hepler, P.K. (1997). Characterization and localization of profilin in pollen grains and tubes of *Lilium longiflorum*. Cell Motil. Cytoskeleton **36,** 323–338.

Villanueva, M.A., Ho, S.-C., and Wang, J.L. (1990). Isolation and characterization of one isoform of actin from cultured soybean cells. Arch. Biochem. Biophys. **277,** 35–41.

Vinh, D.B.-N., and Drubin, D.G. (1994). A yeast TCP-1–like protein is required for actin function in vivo. Proc. Natl. Acad. Sci. USA **91,** 9116–9120.

Weeds, A.G., and Taylor, R.S. (1975). Separation of subfragment-1 isoenzymes from rabbit skeletal muscle myosin. Nature **257,** 54–56.

Xu, P., Lloyd, C.W., Staiger, C.J., and Drøbak, B.K. (1992). Association of phosphatidylinositol 4-kinase with the plant cytoskeleton. Plant Cell **4,** 941–951.

Yen, L.-F., Liu, X., and Cai, S. (1995). Polymerization of actin from maize pollen. Plant Physiol. **107,** 73–76.

Zechel, K., and Weber, K. (1978). Actins from mammals, bird, fish and slime mold characterized by isoelectric focusing in polyacrylamide gels. Eur. J. Biochem. **89,** 105–112.